J|A|C|S
ARTICLES
Published on Web 02/17/2006

Uniquely Strong Electronic Communication between [Mo_2] Units Linked by Dioxolene Dianions

F. Albert Cotton,* Carlos A. Murillo,* Dino Villagrán, and Rongmin Yu

Contribution from the Department of Chemistry and Laboratory for Molecular Structure and Bonding, Texas A&M University, P.O. Box 30012, College Station, Texas 77842-3012

Received December 6, 2005; E-mail: cotton@tamu.edu; murillo@tamu.edu

Abstract: Unprecedented strong electronic communication has been found in dimolybdenum pairs containing quadruply bonded $Mo_2(DAniF)_3^+$ (DAniF = *N*,*N*′-di-*p*-anisylformamidinate) units linked by dioxolene ($C_6X_2O_4^{2-}$) anions. The neutral compounds $[Mo_2(DAniF)_3]_2(C_6X_2O_4)$ (**1**, X = H; **2**, X = Cl; **3**, X = NO_2) and the singly oxidized products $\{[Mo_2(DAniF)_3]_2(C_6X_2O_4)Mo_2\}PF_6$ (**4**, X = H; **5**, X = Cl) have been synthesized and characterized by X-ray crystallography and spectroscopic methods. Unusually short Mo−O distances (~2.05 Å for **1** and **2**, and ~2.01 Å for **4** and **5**) are implicated in the remarkably strong interaction between [Mo_2] units via the linkers. This leads to an extensive charge delocalization in the mixed-valence species, which is mediated by the dioxolene linker, as revealed by the large $\Delta E_{1/2}$ values (763, 795, and 816 mV for **1**, **2**, and **3**, respectively). Additional evidence for the strong electronic coupling is provided by UV−vis, NIR, and EPR spectroscopies and DFT calculations.

Introduction

Mixed-valence (MV) compounds which have two charge-bearing units connected by a linker have been of great interest since the pioneering work on the Creutz−Taube Ru(II)−bridge−Ru(III) compounds.[1] Understanding of the electronic interactions and of electron transfer in such compounds is of fundamental importance in understanding many important chemical and biological processes.[2] The degree of electronic interaction between the metal-based redox centers of such compounds has been investigated in many ways,[1] including the study of their magnetic properties, electrochemistry, and their NIR (near-infrared) or IR spectra.

Most of the studies in this area have focused on systems with single-metal redox centers, generically M−L−M species, that resemble the now famous Creutz−Taube complex. More recently, the range has been extended to dinuclear systems, M_2−L−M_2.[3] In this laboratory, we have found that such species having quadruply bonded $Mo_2(DAniF)_3^+$ units (where DAniF = *N*,*N*′-di-*p*-anisylformamidinate, and the dimolybdenum unit is represented by [Mo_2]) can be prepared readily from precursors, such as $Mo_2(DAniF)_3Cl_2$, $Mo_2(DAniF)_3(OAc)$, or $[Mo_2(DAniF)_3(CH_3CN)_2]^+$, which have immobile outer ligands and bridges that may be inorganic anions, for example, MO_4^{2-} (M = S, Mo, W)[4] and $M(OR)_4^{2-}$ (M = Zn, Co),[5] or organic anions, such as dicarboxylates,[6] diamidates,[7] and cyclic polyamidates.[8] All these compounds have been studied by electrochemistry, whereby the effectiveness of the electronic interaction between the [Mo_2] units has been assessed in terms of the potential difference between the two successive one-electron oxidation processes, $\Delta E_{1/2}$. Previous to this report, the $\Delta E_{1/2}$ values in $[Mo_2]_2L$ compounds have been found in the range from <100 mV for [Mo_2] units linked by saturated dicarboxylate-linked molecules[6a] to as high as 560 mV for β-type oxamidate-linked molecules.[7b,c] However, it is only the β-type oxamidate-linked molecules that unequivocally belong to Class III, according to the Robin−Day classification.[9] Such classifica-

(1) See for example: (a) Creutz, C. *Prog. Inorg. Chem.* **1983**, *30*, 1. (b) Richardson, D. E.; Taube, H. *Coord. Chem. Rev.* **1984**, *60*, 107. (c) Chen, P.; Meyer, T. J. *Chem. Rev.* **1998**, *98*, 1439. (d) Ferretti, A.; Lami, A.; Murga, L. F.; Shehadi, I. A.; Ondrechen, M. J.; Villani, G. *J. Am. Chem. Soc.* **1999**, *121*, 2594. (e) Kaim, W.; Klein, A.; Gloeckle, M. *Acc. Chem. Res.* **2000**, *33*, 755. (f) Demadis, K. D.; Hartshorn, C. M.; Meyer, T. J. *Chem. Rev.* **2001**, *101*, 2655. (g) Brunschwig, B. S.; Creutz, C.; Sutin, N. *Chem. Soc. Rev.* **2002**, *31*, 168. (h) Lau, V. C.; Berben, L. A.; Long, J. R. *J. Am. Chem. Soc.* **2002**, *124*, 9042.

(2) See for example: (a) Prassides, K., Ed. *Mixed-valency Systems: Applications in Chemistry, Physics and Biology*; Kluwer Academic Publishers: Dordrecht, The Netherlands, 1991. (b) Cembran, A.; Bernardi, F.; Olivucci, M.; Garavelli, M. *Proc. Natl. Acad. Sci. U.S.A.* **2005**, *102*, 6255. (c) Talukdar, P.; Bollot, G.; Mareda, J.; Sakai, N.; Matile, S. *J. Am. Chem. Soc.* **2005**, *127*, 6528. (d) Fiedler, A. T.; Bryngelson, P. A.; Maroney, M. J.; Brunold, T. C. *J. Am. Chem. Soc.* **2005**, *127*, 5449. (e) Sakharov, D. V.; Lim, C *J. Am. Chem. Soc.* **2005**, *127*, 4921. (f) Efimov, I.; McIntire, W. S. *J. Am. Chem. Soc.* **2005**, *127*, 732. (g) O'Neill, M. A.; Dohno, C.; Barton, J. K. *J. Am. Chem. Soc.* **2004**, *126*, 1316. (h) Lewis, F. D.; Wu, Y.; Zhang, L.; Zuo, X.; Gayes, R. T.; Wasielewski, M. R. *J. Am. Chem. Soc.* **2004**, *126*, 8206. (i) Wan, C.; Fiebig, T.; Schiemann, O.; Barton, J. K.; Zewail, A. H. *Proc. Natl. Acad. Sci. U.S.A.* **2000**, *97*, 14052. (j) Hess, S.; Götz, M.; Davis, W. B.; Michel-Beyerle, M. E. *J. Am. Chem. Soc.* **2001**, *123*, 10046.

(3) (a) Cotton, F. A.; Lin, C.; Murillo, C. A. *Acc. Chem. Res.* **2001**, *34*, 759. (b) Cotton, F. A.; Lin, C.; Murillo, C. A. *Proc. Natl. Acad. Sci. U.S.A.* **2002**, *99*, 4810. (c) Chisholm, M. H.; Macintosh, A. M. *Chem. Rev.* **2005**, *105*, 2949.

(4) Cotton, F. A.; Donahue, J. P.; Murillo, C. A. *Inorg. Chem.* **2001**, *40*, 2229.

(5) (a) Cotton, F. A.; Liu, C. Y.; Murillo, C. A.; Wang, X. *Inorg. Chem.* **2003**, *42*, 4619. (b) Cotton, F. A.; Dalal, N. S.; Liu, C. Y.; Murillo, C. A.; North, J. M.; Wang, X. *J. Am. Chem. Soc.* **2003**, *125*, 12945.

(6) (a) Cotton, F. A.; Donahue, J. P.; Lin, C.; Murillo, C. A. *Inorg. Chem.* **2001**, *40*, 1234. (b) Cotton, F. A.; Donahue, J. P.; Murillo, C. A. *J. Am. Chem. Soc.* **2003**, *125*, 5436. (c) Cotton, F. A.; Donahue, J. P.; Murillo, C. A.; Pérez, L. M. *J. Am. Chem. Soc.* **2003**, *125*, 5486.

(7) (a) Cotton, F. A.; Daniels, L. M.; Donahue, J. P.; Liu, C.-Y.; Murillo, C. A. *Inorg. Chem.* **2002**, *41*, 1354. (b) Cotton, F. A.; Liu, C. Y.; Murillo, C. A.; Villagrán, D.; Wang, X. *J. Am. Chem. Soc.* **2003**, *125*, 13564. (c) Cotton, F. A.; Liu, C. Y.; Murillo, C. A.; Villagrán, D.; Wang, X. *J. Am. Chem. Soc.* **2004**, *126*, 14822.

(8) Cotton, F. A.; Donahue, J. P.; Murillo, C. A.; Pérez, L. M.; Yu, R. *J. Am. Chem. Soc.* **2003**, *125*, 8900.

tion was consistent with the X-ray structures, electrochemistry, and NIR spectra of the singly oxidized cationic species.

The magnitude of the electronic communication in the $[Mo_2]L[Mo_2]$ species is determined by two factors, namely, the distance between the two $[Mo_2]$ units and the nature of the linker. The idea that led to the work reported here is that noninnocent ligands, such as 2,5-dihydroxy-1,4-benzoquinone (H_2dhbq), also known as anilic acid, and its analogues might be expected to favor the formation of Class III compounds because they have extended π^* orbitals with energies comparable to those of orbitals in transition metals.[10]

The compound H_2dhbq and its analogues belong to a family of versatile multifunctional ligands, and many mononuclear metal complexes containing such ligands have been synthesized.[11] These ligands provide a variety of binding sites to metal cations in various oxidation states. However, because the dhbq moiety can itself bear charges of -1 to -4, assignment of oxidation states of the metal atoms is not trivial. Thus, when a metal complex having a coordinated dhbq ligand is involved in redox chemistry, there is often uncertainty as to whether the redox process takes place at the ligand or at the metal center. For example, $[Co_2(dhbq)(tdpme)_2](BF_4)_2$ ($tdpme_2 = CH_3C(CH_2PPh_2)_3$) which was made from a reaction of $Co(II)(BF_4)_2 \cdot 6H_2O$, tdpme ligand, and H_2dhbq[10] can in principle be formulated in several ways: $[Co(III)(dhbq^{4-})Co(III)]^{2+}$, $[Co(III)(dhbq^{3-})Co(II)]^{2+}$, and $[Co(II)(dhbq^{2-})Co(II)]^{2+}$. The C−O bond distances (1.313(8) and 1.311(8) Å), which are longer than in $dhbq^{2-}$,[12] are consistent with the absence of a delocalized quinoid structure, but because of the lack of structural data for the radical form and the catecholate form and the relatively small change of the geometric parameters of mononuclear metal units in different oxidation states, the exact charges cannot be unequivocally defined. Thus, more for convenience than out of certainty, this species has been described as $[Co(III)(dhbq^{4-})Co(III)]^{2+}$.[10]

Although numerous transition metal complexes with $dhbq^{2-}$ and its analogues have been prepared,[11] these ligands have seldom been used with paddlewheel compounds containing metal−metal bonds.[13] We present here a study on the electronic communication between dimolybdenum units in compounds using as linkers the dianions of 2,5-dihydroxy-1,4-benzoquinone (H_2dhbq, **I**) and its analogues derived from chloranilic acid (H_2ca, **II**) and nitranilic acid (H_2na, **III**) (see Scheme 1). The synthesis, structures, electrochemistry, and electronic structures for the neutral compounds $[Mo_2(DAniF)_3]_2(C_6X_2O_4)$ (**1**, X = H; **2**, X = Cl; **3**, X = NO_2) as well as the structures, spectra (UV−vis and EPR), and magnetic measurements on the singly oxidized molecular pairs $\{[Mo_2(DAniF)_3]_2(C_6X_2O_4)\}PF_6$ (**4**, X=H; **5**, X = Cl) are presented and discussed in this report. It is shown that dioxolene anions provide unprecedented strong electronic communication between $[Mo_2]$ units that involves delocalization of electrons from the linker and those from the metal−metal bonds.

Scheme 1

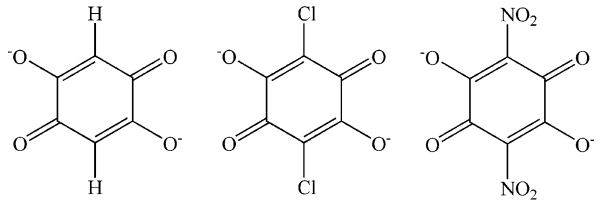

I II III

Experimental Section

All procedures were performed under N_2 using either a N_2 drybox or standard Schlenk line techniques. Solvents were distilled and/or degassed immediately prior to use; acetonitrile was twice distilled under N_2, first from activated molecular sieves and then from CaH_2; CH_2Cl_2, Et_2O, and hexanes were purified under argon using a Glass Contour solvent purification system. The dinuclear precursors $Mo_2(DAniF)_3Cl_2$[14] and $Mo_2(DAniF)_3(O_2CCH_3)$[7c] were prepared by literature methods. Other reagents were purchased from commercial sources and used after degassing but without further purification.

Physical Methods. Elemental analyses were performed by Canadian Microanalytical Service, Delta, British Columbia, upon crystalline samples that were placed overnight under vacuum. Occasionally, residual solvent remained after this process, as indicated by ^{1}H NMR spectroscopy. In such cases, the residual solvent was factored into the elemental analysis. ^{1}H NMR spectra were recorded on an Inova NMR 300 spectrometer with chemical shifts referenced to the protonated solvent residual. Absorption spectra in the range of 250−900 nm were measured at room temperature in degassed CH_2Cl_2 using a Shimadzu UV-2501 PC spectrophotometer. Absorption spectra above 900 nm were obtained in degassed CH_2Cl_2 using a Cary 17 UV−vis spectrophotometer. EPR spectra were recorded using a Bruker ESP300 spectrometer, and the simulations of the spectra were performed using the program WIN-EPR SimFonia from Bruker. Cyclic voltammograms (CVs) and differential pulse voltammograms (DPVs) were recorded using a CH Instruments Model-CH1620A electrochemical analyzer in 0.1 M Bu_4NPF_6 solution in CH_2Cl_2 with Pt working and auxiliary electrodes, a Ag/AgCl reference electrode, and a scan rate of 100 mV/s (CV) or pulse amplitude of 50 mV (DPV). For the DPVs, the increment was 4 mV, the pulse width was 0.05 s, the sample width was 0.0167 s, and the pulse period was 0.2 s. All the potential values are referenced to the Ag/AgCl electrode, and under the present experimental conditions, the $E_{1/2}$ for the Fc^+/Fc couple consistently occurred at +440 mV in CH_2Cl_2.

Preparation of $[Mo_2(DAniF)_3]_2(C_6H_2O_4)$ (1). In a Schlenk flask, a mixture of $H_2C_6H_2O_4$ (35 mg, 0.25 mmol) and excess *n*-butylamine, Bu^nNH_2 (0.15 mL), in 10 mL of methanol was stirred for 5 min. The mixture was then placed under vacuum to remove the solvent and excess Bu^nNH_2. The solid was dissolved in 20 mL of ethanol. In a separate flask, a mixture of $Mo_2(DAniF)_3Cl_2$ (515 mg, 0.500 mmol) and Zn powder (5.0 g) in 50 mL of CH_3CN was stirred for 2 h. The excess Zn was removed by filtration. The filtrate was transferred into the flask containing the ethanol solution of $(Bu^nNH_3)_2C_6H_2O_4$. The mixture was stirred for 2 h at ambient temperature, resulting in the formation of a black−green precipitate. After filtration, the solid was extracted with 15 mL of CH_2Cl_2. The extract was layered with 30 mL of ether. Dark-green crystals of the product were isolated after a period of 1 week. Yield: 250 mg, 49%. ^{1}H NMR (in $CDCl_3$, ppm): δ 6.604 (32H, aromatic C−H), 6.390 (d, 8 H, aromatic C−H), 6.193 (broad, 8H, aromatic C−H), 3.685 (s, 24 H, $-OCH_3$), 3.629 (s, 12H, $-OCH_3$).

(9) Robin, M.; Day, P. *Adv. Inorg. Chem. Radiochem.* **1967**, *10*, 247.
(10) (a) Heinze, K.; Huttner, G.; Zsolnai, L.; Jacobi, A.; Schober, P. *Chem.—Eur. J.* **1997**, *3*, 732. (b) Heinze, K.; Huttner, G.; Walter, O. *Eur. J. Inorg. Chem.* **1999**, 593.
(11) See for example: Kitagawa, S.; Kawata, S. *Coord. Chem. Rev.* **2002**, *224*, 11 and references therein.
(12) Semmingsen, D. *Acta Chem. Scand. B* **1977**, *31*, 11.
(13) Recently, there have been some reports of the use of catecholate ligands in Ru_2^{n+} compounds, but these contain only one diruthenium unit and each ligand is bonded equatorially to one Ru atom. See: (a) Chang, H.-C.; Mochizuki, K.; Kitagawa, S. *Inorg. Chem.* **2005**, *44*, 3799. (b) Chang, H.-C.; Mochizuki, K.; Kitagawa, S. *Inorg. Chem.* **2005**, *44*, 3810.
(14) Cotton, F. A.; Daniels, L. M.; Jordan, G. T., IV; Lin, C.; Murillo, C. A. *J. Am. Chem. Soc.* **1998**, *120*, 3398.

Absorption spectrum (CH_2Cl_2) λ_{max} (ϵ_M, M^{-1} cm^{-1}): 284 nm (1.26×10^5), 362 nm (3.76×10^4), 716 nm (7.40×10^3), 852 nm (6.40×10^3), 970 nm (8.20×10^3), 1128 nm (2.30×10^4). Anal. Calcd for $C_{96}H_{92}Mo_4N_{12}O_{16}\cdot CH_2Cl_2$: C, 54.28; H, 4.42; N, 7.84%. Found: C, 54.32; H, 4.45; N, 7.69%.

Preparation of $[Mo_2(DAniF)_3]_2(C_6Cl_2O_4)$ (2). A suspension of $Mo_2(DAniF)_3(CH_3CO_2)$ (460 mg, 0.433 mmol) and H_2ca (42 mg, 0.20 mmol) in 30 mL of CH_3CN was refluxed for 3 h using a Soxhlet extractor with K_2CO_3 in the thimble to scavenge the acetic acid that was produced. After cooling, the green solid was isolated by filtration, washed with 2 × 20 mL of ethanol, dried in vacuum, dissolved in 100 mL of CH_2Cl_2, and filtered again. The solution was then layered with 200 mL of ether. Dark-green crystals of the product were obtained after a week. Yield: 195 mg, 40%. ^{1}H NMR (in $CDCl_3$, ppm): δ 8.671 (s, 2H, −NCHN−), 8.398 (s, 4H, −NCHN−), 6.804 (d, 16H, aromatic C−H), 6.627 (d, 16 H, aromatic C−H), 6.349 (d, 8H, aromatic C−H), 6.119 (d, 8H, aromatic C−H), 3.686 (s, 24 H, $-OCH_3$), 3.600 (s, 12H, $-OCH_3$). Absorption spectrum (CH_2Cl_2) λ_{max} (ϵ_M, M^{-1} cm^{-1}): 285 nm (1.08×10^5), 378 nm (2.68×10^4), 729 nm (2.81×10^3), 857 nm (4.86×10^3), 1185 nm (2.66×10^4). Anal. Calcd for $C_{976}H_{90}N_{12}Cl_2O_{16}Mo_4\cdot 1.5CH_2Cl_2$: C, 51.90; H, 4.16; N, 7.45%. Found: C, 51.91; H, 3.66; N, 7.45%.

Preparation of $[Mo_2(DAniF)_3]_2(C_6(NO_2)_2O_4)$ (3). This green compound was made similarly to **2** using $Mo_2(DAniF)_3(CH_3CO_2)$ (1.02 g, 1.00 mmol) and H_2na (115 mg, 0.50 mmol). Yield: 208 mg, 19%. ^{1}H NMR (in $CDCl_3$, ppm): δ 8.771 (s, 2H, −NCHN−), 8.497 (s, 4H, −NCHN−), 6.680 (dd, 32H, aromatic C−H), 6.328 (d, 8H, aromatic C−H), 6.127 (d, 8H, aromatic C−H), 3.688 (s, 24 H, $-OCH_3$), 3.589 (s, 12H, $-OCH_3$). Absorption spectrum (CH_2Cl_2) λ_{max} (ϵ_M, M^{-1} cm^{-1}): 281 nm (1.0×10^5), 365 nm (2.59×10^4), 677 nm (2.97×10^3), 805 nm (3.22×10^3). Anal. Calcd for $C_{96}H_{90}Mo_4N_{14}O_{20}\cdot 3CH_2Cl_2$: C, 49.46; H, 4.03; N, 8.16%. Found: C, 48.93; H, 4.19; N, 8.19%.

Preparation of $\{[Mo_2(DAniF)_3]_2(C_6H_2O_4)\}PF_6$ (4). A mixture of compound **1** (250 mg, 0.120 mmol) and Cp_2FePF_6 (50 mg, 0.15 mmol) in 30 mL of THF was stirred for 1 day at ambient temperature. After filtration, the solid residue was extracted with 30 mL of CH_2Cl_2. The extract was then layered with 40 mL of diethyl ether over a period of a week. The dark-green crystalline product was isolated by filtration, washed with 2 × 20 mL of ether, and then dried in vacuum. Yield: 120 mg, 44%. Absorption spectrum (CH_2Cl_2) λ_{max} (ϵ_M, M^{-1} cm^{-1}): 281 nm (7.16×10^4), 400 nm (3.08×10^4), 591 nm (1.01×10^3), 852 nm (1.08×10^5). Anal. Calcd for $C_{96}H_{92}N_{12}PF_6O_{16}Mo_4$: C, 52.24; H, 4.20; N, 7.62%. Found: C, 52.09; H, 3.97; N, 7.56%.

Preparation of $\{[Mo_2(DAniF)_3]_2(C_6Cl_2O_4)\}PF_6$ (5). A mixture of compound **2** (310 mg, 0.15 mmol) and $AgPF_6$ (75 mg, 0.30 mmol) in 30 mL of THF was stirred overnight. After filtration, the very dark-green residue was extracted with 30 mL of CH_2Cl_2. The extract was then layered with 40 mL of diethyl ether over a period of a week. The crystalline product was isolated by filtration, washed with 2 × 20 mL of ether, and then dried in vacuum. Yield: 275 mg, 81%. Absorption spectrum (CH_2Cl_2) λ_{max} (ϵ_M, M^{-1} cm^{-1}): 282 nm (1.02×10^{45}), 421 nm (3.81×10^4), 592 nm (7.97×10^2), 840 nm (1.29×10^5). Anal. Calcd for $C_{96}H_{90}N_{12}Cl_2PF_6O_{16}Mo_4$: C, 50.68; H, 3.99; N, 7.39%. Found: C, 50.76; H, 4.11; N, 7.48%.

Computational Details. Density functional theory (DFT)[15] calculations were performed with the hybrid Becke-3 parameter[16] exchange functional and the Lee−Yang−Parr[17] nonlocal correlation functional (B3LYP) implemented in the Gaussian 03 program suite.[18] Double-ζ quality basis sets (D95)[19] were used on nonmetal atoms (carbon, nitrogen, oxygen, and hydrogen). A small (1s2s2p3s3p3d) effective core potential (ECP)[20] was used for the molybdenum atoms along with the associated double-ζ basis set (LANL2DZ). The convergence criterion for the self-consistent field cycles on all calculations was increased from the default value to 10^{-8}. Time-dependent calculations were also performed to assign the electronic spectra. All calculations were done on an Origin 3800 64-processor SGI computer located at the Texas A&M supercomputing facility.

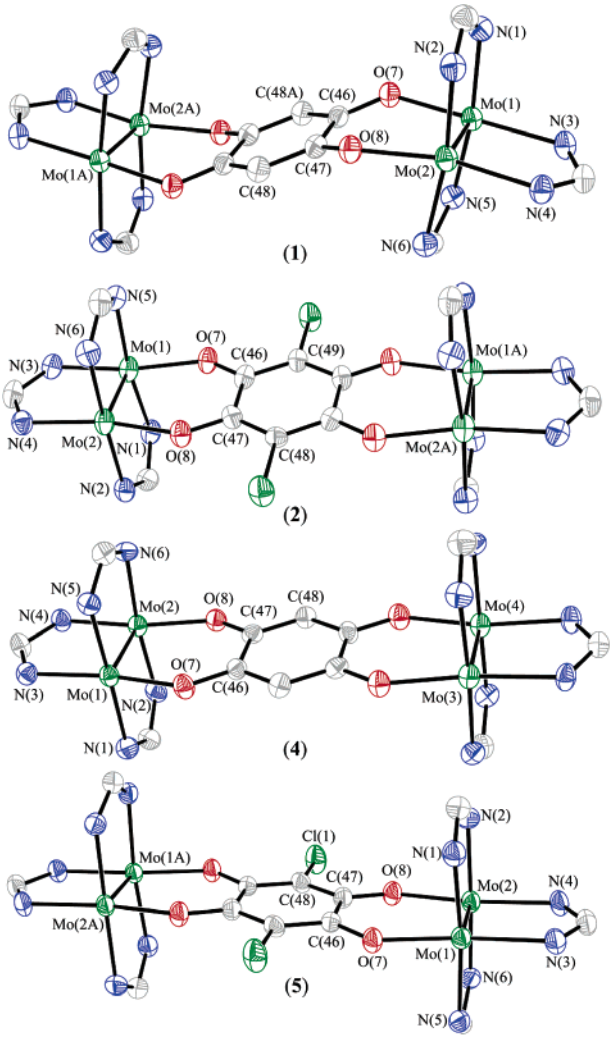

Figure 1. The core structures of compounds **1** and **2** and the cations in **4** and **5**. Displacement ellipsoids are drawn at the 50% probability level. The *p*-anisyl groups attached to the N atoms and all hydrogen atoms are omitted for clarity.

X-ray Structure Determinations. Data were collected at −60 °C on a Bruker SMART 100 CCD area detector. Cell parameters were determined using the program SMART.[21] Data reduction and integration were performed with the software package SAINT,[22] while absorption corrections were applied by using the program SADABS.[23] The positions of the Mo atoms were found by direct methods using the program package SHELXTL.[24] Alternating cycles of least-squares refinement followed by difference Fourier syntheses revealed the positions of the remaining non-hydrogen atoms. Hydrogen atoms were not included in the structure refinement. All non-hydrogen atoms, except those disordered in **2**, were refined with anisotropic displacement coefficients.

In **2**, a *p*-anisyl group shows two orientations with 0.53 and 0.47 occupancies. The details of data collection and refinement for all compounds are listed in Table 1. The core structures of these compounds are presented in Figure 1. Selected bond distances and angles are listed in Table 2 for compounds **1**, **2**, **4**, and **5**.

(15) (a) Hohenberg, P.; Kohn, W. *Phys. Rev.* **1964**, *136*, B864. (b) Parr, R. G.; Yang, W. *Density-Functional Theory of Atoms and Molecules*; Oxford University Press: Oxford, 1989.
(16) (a) Becke, A. D. *Phys. Rev. A* **1988**, *38*, 3098. (b) Becke, A. D. *J. Chem. Phys.* **1993**, *98*, 1372. (c) Becke, A. D. *J. Chem. Phys.* **1993**, *98*, 5648.
(17) Lee, C. T.; Yang, W. T.; Parr, R. G. *Phys. Rev. B* **1998**, *37*, 785.
(18) Frisch, M. J.; et. al. *Gaussian 98*, revision A.9; Gaussian, Inc.: Pittsburgh, PA, 1998.

Table 1. Crystallographic Data for **1**, **2**, **4**, and **5**

compound	**1**·$2CH_2Cl_2$	**2**·$3CH_2Cl_2$·$2C_2H_5OC_2H_5$	**4**·$2CH_2Cl_2$	**5**·$2CH_2Cl_2$
chemical formula	$C_{98}H_{96}Cl_4Mo_4N_{12}O_{16}$	$C_{103}H_{106}Cl_8Mo_4N_{12}O_{17}$	$C_{98}H_{96}Cl_4F_6Mo_4N_{12}O_{16}P$	$C_{98}H_{94}Cl_6F_6Mo_4N_{12}O_{16}P$
fw	2223.43	2451.36	2368.40	2437.28
crystal system	triclinic	monoclinic	triclinic	triclinic
space group	$P\bar{1}$	$P2_1/m$	$P\bar{1}$	$P\bar{1}$
a (Å)	11.437(1)	12.964(2)	15.892(2)	10.032(2)
b (Å)	13.639(2)	25.107(4)	17.715(2)	15.908(3)
c (Å)	16.180(2)	17.187(3)	20.794(3)	17.854(3)
α (deg)	95.478(2)	90	76.494(3)	110.757(3)
β (deg)	99.144(2)	103.350(3)	67.595(2)	94.391(3)
γ (deg)	104.669(2)	90	72.588(2)	103.410(3)
V (Å^3)	2386.2(5)	5442(2)	5117(1)	2552.1(7)
Z	1	2	2	1
d_{calcd} (g cm^{-3})	1.547	1.496	1.537	1.586
μ(Mo K$_\alpha$) (mm^{-1})	0.698	0.715	0.679	0.734
T, °C	213(2)	213 (2)	213(2)	213(2)
GOF	1.053	1.039	1.009	1.014
$R1$,[a] $wR2$[b] ($I > 2\sigma$)	0.0359, 0.0874	0.0570, 0.1478	0.0543, 0.1241	0.0436, 0.1025

[a] $R1 = [\sum w(F_o - F_c)^2/\sum wF_o^2]^{1/2}$. [b] $wR2 = [\sum [w(F_o^2 - F_c^2)^2]/\sum w(F_o^2)^2]^{1/2}$, $w = 1/[\sigma^2(F_o^2) + (aP)^2 + bP]$, where $P = [\max(F_o^2,0) + 2(F_c^2)]/3$.

Table 2. Selected Bond Distances (Å) and Angles (°) for **1**, **2**, **4**, and **5**

	1	**2**	**4**	**5**
Mo(1)−Mo(2)	2.1051(4)	2.1057(7)	2.1211(7)	2.1260(5)
Mo(1)−N(1)	2.133(3)	2.155(4)	2.145(5)	2.116(3)
Mo(1)−N(3)	2.135(3)	2.116(4)	2.122(4)	2.131(3)
Mo(1)−N(5)	2.146(3)	2.136(4)	2.134(4)	2.119(3)
Mo(2)−N(2)	2.146(3)	2.134(4)	2.135(4)	2.139(3)
Mo(2)−N(4)	2.110(3)	2.115(5)	2.107(4)	2.108(3)
Mo(2)−N(6)	2.154(3)	2.151(4)	2.137(4)	2.137(3)
Mo(1)−O(7)	2.063(2)	2.049(3)	2.025(4)	2.026(2)
Mo(2)−O(8)	2.058(2)	2.049(4)	1.998(4)	2.014(2)
O(7)−C(46)	1.294(4)	1.285(6)	1.308(6)	1.296(4)
O(8)−C(47)	1.297(4)	1.292(6)	1.310(6)	1.302(4)
C(47)−C(48)	1.383(5)	1.380(6)		1.392(5)
C(48)−C(46A)	1.393(4)		1.378(7)	1.392(4)
C(46)−C(47)	1.481(5)	1.390(6)		1.460(5)
C(46A)-C(49)		1.475(7)	1.468(7)	
O(7)−Mo(1)−N(1)	87.1(1)	87.6(2)	88.9(2)	86.7(1)
N(1)−Mo(1)−N(3)	97.6(1)	93.3(2)	91.7(2)	92.2(1)
O(7)−Mo(1)−N(5)	83.8(1)	86.0(2)	88.8(2)	88.0(1)
N(3)−Mo(1)−N(5)	90.6(11)	92.3(2)	89.5(2)	92.3(1)
O(8)−Mo(2)−N(2)	90.5(1)	85.9(2)	87.5(2)	88.0(1)
N(4)−Mo(2)−N(2)	96.6(1)	92.2(2)	92.4(2)	91.9(1)
O(8)−Mo(2)−N(6)	81.1(1)	87.9(2)	87.7(2)	88.6(1)
N(4)−Mo(2)−N(6)	90.8(1)	93.0(2)	91.5(2)	90.6(1)

The quality of the diffraction data for **3** was insufficient for a detailed structural analysis. However, a structural analysis unambiguously shows the existence of a molecular pair composed of two [Mo_2] units and a nitranilate dianions in which the NO_2 groups are perpendicular to the C_6O_4 plane. Since repeated attempts to obtain crystals with better diffraction characteristics have been unsuccessful, only basic crystallographic data are provided.[25] A figure of its core structure is provided as Supporting Information (Figure S1).

Results and Discussion

Syntheses. Because anilic acid (2,5-dihydroxy-1,4-benzoquinone), chloranilic acid (2,5-dihydroxy-3,6-dichloro-1,4-benzoquinone), and nitranilic acid are relatively strong organic acids (pK_1 = 2.71, pK_2 = 5.18 for H_2dhbq, pK_1 = 0.73, pK_2 = 3.08 for H_2ca, and pK_1 = −3.0, pK_2 = −0.5 for H_2na), they can be easily deprotonated using Bu^nNH_2 to produce the corresponding *n*-butylammonium salts. Two methods have been used to make each of the neutral compounds, **1**−**3**, as shown in reactions (1a, 1b) and (2), where H_2L represents one of these acids. In the Experimental Section, we give details of method (1) for **1** and method (2) for **2**.

$$2Mo_2(DAniF)_3Cl_2 + Zn + CH_3CN \rightarrow 2[Mo_2(DAniF)_3(CH_3CN)_2]ZnCl_4 \quad (1a)$$

$$2[Mo_2(DAniF)_3(CH_3CN)_2]^+ + L^{2-} \rightarrow [Mo_2(DAniF)_3]L[Mo_2(DAniF)_3] \quad (1b)$$

$$2Mo_2(DAniF)_3(OAc) + H_2L \rightleftharpoons [Mo_2(DAniF)_3]L[Mo_2(DAniF)_3] \quad (2)$$

The first method is a two-step process that involves reduction of $Mo_2(DAniF)_3Cl_2$ with Zn metal in acetonitrile (eq 1a) followed by an in situ reaction with the corresponding *n*-butylammonium dianion of the linker (eq 1b). The neutral pairs precipitate directly from acetonitrile solutions as green microcrystalline solids that are conveniently isolated by filtration and further purified by recrystallization after layering a solution of the product in CH_2Cl_2 with either diethyl ether or isomeric hexanes. The products are moderately stable to air as solids, but in solution, they decompose readily on exposure to air. Method (1) has been successfully used in the preparations of many [Mo_2]L[Mo_2] compounds in reactions involving H_2L precursors that may be easily deprotonated by a base, such as tetraalkylammonium hydroxide. For the preparation of **1**, Bu^nNH_2 was employed instead of the commonly used R_4NOH bases to avoid generating water, which may then react with the $[Mo_2(DAniF)_3(CH_3CN)_2]^+$ cation generated in situ. This obviates the formation of products with hydroxide or oxo bridges.[26] An additional advantage is that removal of excess Bu^nNH_2 is conveniently achieved under vacuum.

(19) Dunning, T. H.; Hay, P. J. In *Modern Theoretical Chemistry 3. Methods of Electronic Structure Theory*; Schaefer, H. F., III, Ed.; Plenum Press: New York, 1977; pp 1−28.
(20) (a) Wadt, W. R.; Hay, P. J. *J. Chem. Phys.* **1985**, *82*, 284. (b) Wadt, W. R.; Hay, P. J. *J. Chem. Phys.* **1985**, *82*, 299.
(21) *SMART* for Windows NT, version 5.618: Bruker Advanced X-ray Solutions, Inc.: Madison, WI, 2001.
(22) *SAINT*, Data Reduction Software, version 6.36A; Bruker Advanced X-ray Solutions, Inc.: Madison, WI, 2001.
(23) *SADABS*, Area Detector Absorption and other Corrections Software, version 2.05; Bruker Advanced X-ray Solutions, Inc.: Madison, WI, 2000.
(24) Sheldrick, G. M. *SHELXTL*, version 6.12; Advanced X-ray Solutions, Inc.: Madison, WI, 2002.
(25) Crystallographic data for **3**: space group *C*2/*m*, a = 17.35(1) Å, b = 25.45(2) Å, c = 12.888(8) Å, β = 103.52(1)°, V = 5532(6) Å^3, Z = 2, $R1$ = 0.1259.
(26) Cotton, F. A.; Daniels, L. M.; Guimet, I.; Henning, R. W.; Jordan, G. T., IV; Lin, C.; Murillo, C. A.; Schultz, A. J. *J. Am. Chem. Soc.* **1998**, *120*, 12531.

The second method uses $Mo_2(DAniF)_3(OAc)$ as the [Mo_2] precursor. This method is quite convenient because this dimolybdenum starting material[7c] can be synthesized in high yield and more easily than $Mo_2(DAniF)_3Cl_2$. This mixed acetate−formamidinate starting material has previously been used to synthesize compounds with bridges whose precursors cannot be deprotonated with tetraalkylammonium hydroxide, such as dimethyloxamine.[7] Because the reactions in method (2) are reversible, a Soxhlet apparatus with a K_2CO_3 trap is used to remove the byproduct, acetic acid, and drive the reaction in the forward direction.

The singly oxidized compound **4**, $\{[Mo_2(DAniF)_3]_2(C_6H_2O_4)\}PF_6$, was prepared in good yield by reacting the neutral species, **1**, with excess $FeCp_2PF_6$ or an equivalent amount of a silver salt in THF, while compound **5** was obtained using 2 equiv of $AgBF_4$ as the oxidizing reagent.[27] These reactions were carried out at room temperature by stirring for over a period of 24 h. Compounds **4** and **5** are stable to air in the solid state.[28] Efforts to isolate the doubly oxidized species of compounds **1** and **2** have been unrewarding.

Crystal Structures. Compound **1** crystallizes in the triclinic space group $P\bar{1}$ with $Z = 1$ with two interstitial CH_2Cl_2 molecules per bridged molecule. The [Mo_2] units are related by an inversion center, and the Mo−Mo bond distance, 2.1051(4) Å, is in the normal range for quadruply bonded compounds.[29] The two Mo−Mo bonds are parallel, and the distance between their midpoints is 8.536 Å. The Mo−O distances, 2.063(2) and 2.058(2) Å, are significantly shorter than those in compounds with other O-donor linkers. For example, the average Mo−O distances in $Mo_2(DAniF)_3(C_2O_4)Mo_2(DAniF)_3$ are 2.130(4) Å,[6a] and it is 2.114(3) Å in $Mo_2(DAniF)_3(CH_3N(O)CC(O)NCH_3)Mo_2(DAniF)_3$.[7c] However, the average Mo−N distance in **1**, 2.137(6) Å, is within the usual range. The $dhbq^{2-}$ dianion is essentially planar, but the two Mo_2 units are located about 0.8 Å above and below the plane, which results in the formation of a chair conformation for the [Mo_2](dhbq)[Mo_2] fragment. The dihedral angle between the ligand plane and the O−Mo−Mo−O plane is 155.9°. The idealized symmetry in the structure is C_{2h}.

The six-membered ring formed by the carbon atoms in the $dhbq^{2-}$ ligand shows large variations in C−C distances, as indicated in Scheme 2a. The two crystallographically independent *A* distances, 1.383(5) and 1.393(4) Å, have values similar to those in an aromatic phenyl ring, but the *B* distances, 1.481(5) Å, have a value that is close to the single bond (1.51(1) Å) in an oxalate group.[6a] The large differences in C−C distances within the ring show that the electrons are not delocalized within the six-membered ring. Interestingly, the *C* distances, 1.294(4) and 1.297(4) Å, are longer than typical C═O double bonds but shorter than those for C−O single bonds, suggesting that there is electron delocalization in the O−C−C(H)−C−O groups. Additionally, the very short Mo−O distances (average 2.011 Å) indicate that there is a strong interaction with the Mo_2 units, and it appears that the electron delocalization extends through the 14-atom ring that includes the linker and the four Mo atoms of the two dimolybdenum units, as shown schematically in Scheme 2b. This resembles a heteroanthracene in which there is large delocalization within the ring but lesser communication through the *B* bonds.[30]

Scheme 2

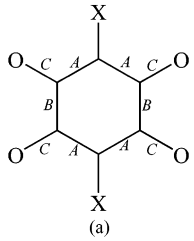

(a)

For **1**, A = 1.386(3), 1.392(3) Å; B = 1.481(4) Å; and C = 1.295(3), 1.296(3) Å. For **2**, A = 1.380(6), 1.390(6) Å; B = 1.475(7) Å; and C = 1.285(6), 1.292(6) Å.

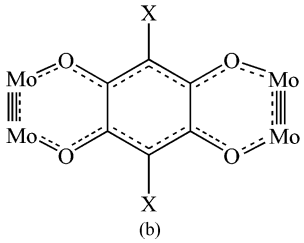

(b)

X = H (**1**), or Cl (**2**)

When the linker is the dianion of chloranilic acid, the neutral product (**2**) crystallizes in the space group of $P2_1/m$ with $Z = 2$, and the [Mo_2] units are related by a crystallographic plane of symmetry. This structure is similar to that of **1**, and it can also be described as a delocalized $(O-C-C(Cl)-C-O)_2(Mo_2)_2$ group (Scheme 2). Whereas the bond distances in **2** are nearly the same to the respective ones in **1**, the conformations of these two compounds are different. In **2**, the central [Mo_2](L)[Mo_2] fragment is essentially flat in contrast to the chair-type structure in **1**, and this is reflected in an increase of 0.2 Å in the distance between the midpoints of the two Mo−Mo bonds (8.718 Å). It is interesting that the difference of the overall conformation of the [Mo_2](L)[Mo_2] fragment does not influence the Mo−Mo (2.1057(7) Å) and Mo−O (2.049(3) and 2.050(5) Å) bond distances as these values are essentially the same as those in **1**. In the two compounds, the Mo−Mo bonds are parallel to each other.

In the singly oxidized compound **4**, the core structure is flat, in contrast to the chair conformation in the neutral precursor. Compound **4** crystallizes in the space group $P\bar{1}$ with $Z = 2$; thus, the entire cation is the asymmetric unit. In this mixed-valence compound, the distance between the midpoints of the two Mo−Mo bonds decreases to 8.616 Å. Again, the two crystallographically independent Mo−Mo bonds (2.1211(7) and 2.1194(7) Å) are parallel to each other. These distances are chemically equivalent and about 0.015 Å longer than those in **1**. These features are consistent with the removal of one δ bonding electron and concomitant delocalization of the unpaired electron over the two [Mo_2] units.

(27) Use of 2 equiv of $AgBF_4$ was necessary to produce satisfactory crystals for X-ray analysis even though contamination with the doubly oxidized species in solution is expected from the CV. When 1 equiv of the oxidizing agent was used, the crystals showed a poor diffraction pattern. However, we found that, for spectroscopic studies in the near-IR, the use of 1 equiv of the oxidizing agent is adequate.

(28) It should be noted that chemical oxidation of **3** was not attempted.

(29) Cotton, F. A. In *Multiple Bonds Between Metal Atoms*, 3rd ed.; Cotton, F. A., Murillo, C. A., Walton, R. A., Eds.; Springer Science and Business Media, Inc.: New York, 2005.

(30) A similar situation is also apparent in polyacenes, such as pentacene. See for example: (a) Anthony, J. E.; Brooks, J. S.; Eaton, D. L.; Parkin, S. R. *J. Am. Chem. Soc.* **2001**, *123*, 9482. (b) Tantillo, D. J.; Hoffmann, R.; Houk, K. N.; Warner, P. M.; Brown, E. C.; Henze, D. K. *J. Am. Chem. Soc.* **2004**, *126*, 4256.

Table 3. Electrochemical Data for Selected $[Mo_2(DAniF)_3](L)[Mo_2(DAniF)_3]$ Compounds[a]

L	$E_{1/2}(0/-1)$ (mV)[b]	$E_{1/2}(+1/0)$ (mV)	$E_{1/2}(+2/+1)$ (mV)	$\Delta E_{1/2}$ (mV)[c]	K_C[d]	ref
$dhbq^{2-}$ (**1**)	−1115	−200	563	763	7.92×10^{12}	this work
ca^{2-} (**2**)	−940	−15	780	795	2.75×10^{13}	this work
na^{2-} (**3**)	−827	45	861	816	6.23×10^{13}	this work
$^{-}O_2CCO_2^{-}$		260	472	223	5.9×10^{3}	6a
$^{-}O_2CCH_2CO_2^{-}$		225	285	108	67	6a
$^{-}O_2CCH_2CH_2CO_2^{-}$		225	285	100	49	6a
α-diphenyloxamidate		176	367	191	1.7×10^{3}	7b
β-diphenyloxamidate		−157	383	540	1.3×10^{9}	7b
β-dimethyloxamidate		−169	362	531	9.5×10^{8}	7c
$(H)_2^{2-}$		165	1048	883	8.46×10^{14}	39

[a] All potentials are referenced to Ag/AgCl. [b] $E_{1/2} = E_{1/2}(E_{pa} + E_{pc})/2$ from the CV for compounds **1** and **2**, while $E_{1/2} = E_p + E_{pul}/2$ and $E_{pul} = 25$ mV from DPV for compound **3**. [c] $\Delta E_{1/2}$ is for the metal-based redox steps. [d] K_C is calculated using the formula $K_C = \exp(\Delta E_{1/2}/25.69)$.

The average Mo−O distance (2.011(8) Å) is about 0.05 Å shorter than that in the precursor, **1**. The shortening is partially due to the increase of positive charge in the $[Mo_2]$ units, but electronic contributions are also expected because the bonding between the Mo and O atoms in **1** has antibonding character in the HOMO (vide infra). It is interesting to note that there is no significant change in the average Mo−N distance (2.13(1) and 2.137(6) Å for compounds **1** and **4**, respectively).

It should be noted that the structural dimensions of the $dhbq^{2-}$ dianion in both **1** and **4** are the same within experimental error. The average distances are 1.307(13) Å for the C−O bonds, 1.466(10) Å for the single C−C bond, and 1.384(14) Å for the delocalized C−C bonds. This invariance strongly supports a metal-based oxidation rather that a linker-based oxidation.

Compound **5** crystallizes in the space group $P\bar{1}$ with $Z = 1$. The $[Mo_2]$ units of the cation are equal because they are related by a crystallographic inversion center. The independent Mo−Mo distance (2.1260(5) Å) is about 0.020 Å longer than that in the precursor **2**. The distance between midpoints of the two Mo−Mo bonds is 8.651 Å. The average Mo−O distance (2.020(3) Å) is about 0.03 Å shorter than that in compound **2**. Similarly to **4**, the average of Mo−N distance (2.122(7) Å) does not change relative to that in the precursor. The structural parameters of the dianion linker are again very close to those in the neutral compound **2**. In the crystal, the overall core structure of **5** is not as flat as that in **2**, and the $[Mo_2]$ units are 0.17 Å above or below the plane of the bridging ligand. The reason for such conformational difference is not clear, but the influence of packing forces cannot be ruled out.

Electrochemistry, EPR, and DFT Calculations. The electrochemical behavior of the neutral compounds **1**−**3** and the EPR spectra of the MV species **4** and **5** have been investigated. Additionally, DFT calculations for **1** and the cation of **4** with models in which the *p*-anisyl groups in the formamidinate ligands were replaced by hydrogen atoms, namely, $[Mo_2(HNHCHNH)_3]_2(C_6H_2O_4)$ and $[Mo_2(HNHCHNH)_3]_2(C_6H_2O_4)]^+$, have been performed to provide further understanding of the electronic interaction between the $[Mo_2]$ units in these compounds and the degree of delocalization of the odd electron in the oxidized species.

Electrochemical data are commonly and conveniently used to classify the mixed-valence compounds according to the Robin and Day classification since cyclic voltammograms and differential pulse voltammograms provide useful information about the degree of the interaction between redox centers.[31] Molecular pairs of the type $[Mo_2]L[Mo_2]$ can be oxidized electrochemically, generally in two successive one-electron redox steps. From the separation of these redox steps ($\Delta E_{1/2}$), the comproportionation constant, K_C, may be calculated. The K_C represents the equilibrium constant for the reaction:

$$[Mo_2]L[Mo_2] + [Mo_2^{+}]L[Mo_2^{+}] \rightleftharpoons 2\{[Mo_2]L[Mo_2]\}^{+}$$

The singly oxidized species on the right-hand side of this equation is presented in a simplified manner in which the entire unit bears a positive charge. How that positive charge is distributed is determined by the strength of the interaction between the two $[Mo_2]$ units. There are two extreme cases for the distribution of the positive charge. In one, the positive charge is carried entirely by one $[Mo_2]$ unit; in other words, the charge is localized and the interaction between $[Mo_2]$ units is very weak. In this case, a second one-electron oxidation should occur on the second $[Mo_2]$ unit, which is neutral. Therefore, the separation of the two successive one-electron redox steps is expected to be small. Additionally, the structure of the monocation should be expected to have two different Mo−Mo distances. In the other extreme case, the positive charge is distributed evenly over the two $[Mo_2]$ units, and each $[Mo_2]$ unit carries a formal charge of +0.5. Therefore, the second one-electron oxidation process is expected at a significantly more positive potential than the first one, and the two Mo−Mo distances should be similar.

Electrochemistry for **1**−**3** (Table 3 and Figure 2) shows three well-separated reversible waves for **1** and **2** in the window provided by the solvent, CH_2Cl_2. For **3**, the process occurring at the most positive potential appears to be irreversible under the same experimental conditions.[32] The features at −1.115, −0.940, and −0.827 V for **1**, **2**, and **3**, respectively, are assigned to a one-electron reduction of the linker by comparison with previous assignments in the literature.[10,33] The other two processes are $[Mo_2]$-centered, and they correspond to the oxidation of each neutral compound to a singly ($[Mo_2]L[Mo_2]^+$) and a doubly oxidized species ($[Mo_2]L[Mo_2]^{2+}$). These assignments are well supported by DFT calculations for the model of **1**. As shown in Figure 3, the HOMO is formed by the in-phase

(31) Cannon, R. D. *Electron-Transfer Reactions*; Butterworth: London, 1980.
(32) The origin of the weak signals that appear between the main peaks in the DPV of **3** is not certain, but it may be due to slight contamination by minor decomposition products.
(33) The appearance of three redox processes in $[Mo_2]L[Mo_2]$ compounds was recently reported for a compound where L = fluoflavinate, in which two redox processes are metal-based and one is ligand-based. See: Cotton, F. A.; Li, Z.; Liu, C. Y.; Murillo, C. A.; Villagrán, D. *Inorg. Chem.* **2006**, *45*, 767.

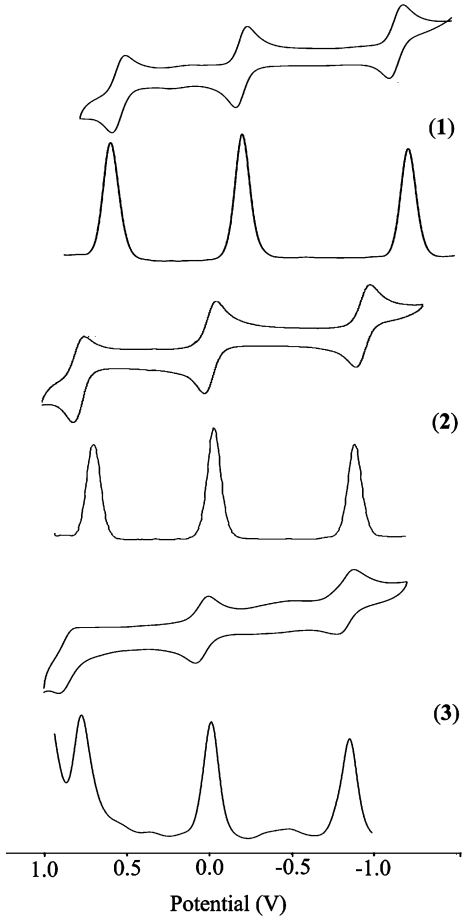

Figure 2. The cyclic voltammograms and the differential pulse voltammograms (below each CV) for **1**−**3**. Data were obtained in CH_2Cl_2 solution with potentials referenced to Ag/AgCl.

combination (b_{1u}) of the δ orbitals of the two [Mo_2] units (in D_{2h} symmetry) interacting with an occupied π^* orbital (b_{1u}) of the linker. The out-of-phase δ combination (b_{2g}) of the [Mo_2] units interacts with an empty π^* orbital (b_{2g}) of the linker to give a low-lying filled orbital (HOMO-1) and the LUMO (Figure 4). The [Mo_2] units make the largest contribution to the HOMO (63%), while the LUMO has mainly ligand character (69%), with a small metal contribution. Furthermore, the metal character of the HOMO agrees with the EPR results for the singly oxidized compounds **4** and **5** (vide infra).

The first oxidation process for the neutral species, at −200 mV for **1**, −15 mV for **2**, and 45 mV for **3**, occurs at lower potentials than for the oxidation of the dicarboxylate analogues (see Table 3), indicating that the HOMOs for **1**−**3** are higher in energy than those for the latter. The redox potentials show a positive shift for **2** and **3** compared with that for **1**, which is consistent with the presence of the electron-withdrawing substituents on the linker in **2** and **3** (Cl and NO_2, respectively). It is interesting that the difference in the first oxidation process between **2** and **3** is only 60 mV, even though the nitro group is potentially a powerful π electron-withdrawing group and it would be expected to strongly influence the oxidation potentials. The relatively small difference is consistent with the structure of **3** (Figure S1) that shows that the NO_2 groups are perpendicular to the $C_6O_4N_2$ plane, thus blocking any potential π interaction. Therefore, the net electron-withdrawing effect from the NO_2 groups in **3** is caused exclusively by σ interactions.

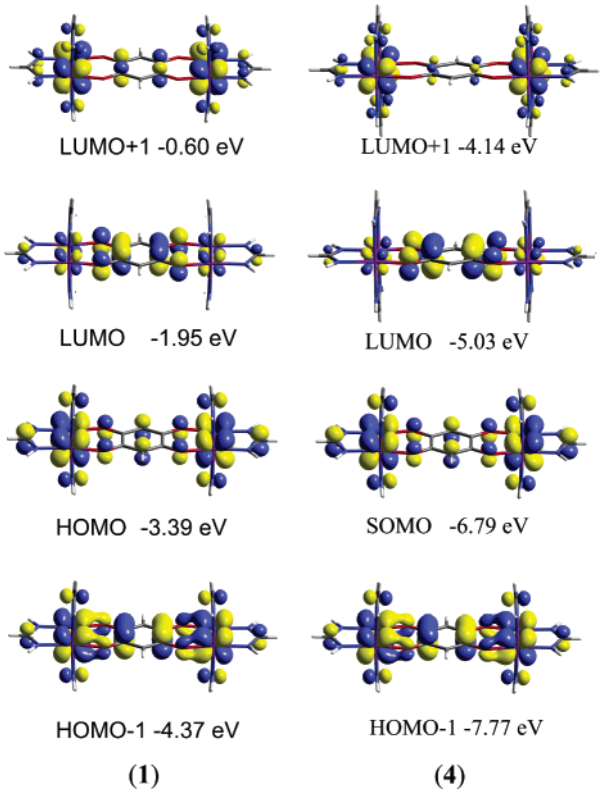

Figure 3. Selected frontier orbital plots calculated for **1** and **4**. Orbitals are drawn using an isosurface value of 0.04.

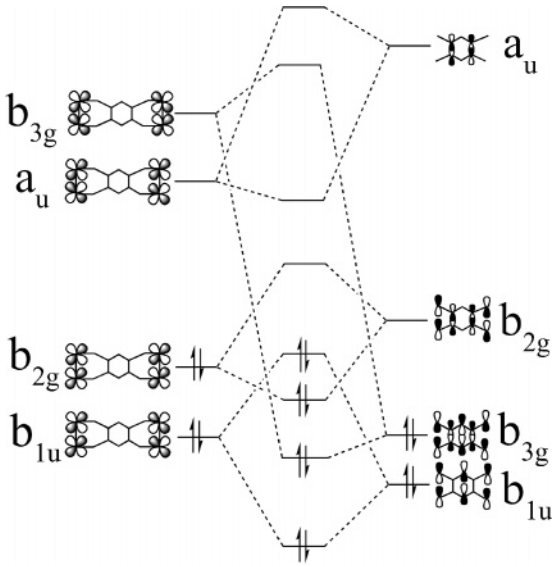

Figure 4. Orbital interaction diagram for **1**. The left column shows the frontier orbitals from the dimetal units, and the right column has the linker orbitals.

The $\Delta E_{1/2}$ values of the two successive [Mo_2]-centered redox steps (763 mV for **1**, 795 mV for **2**, and 816 mV for **3**) are much larger than those for any of the previously reported [Mo_2]L[Mo_2] molecules, such as those with dicarboxylates and diamidates. This is evident in Figure 5. When these values are used to calculate the K_C values using the expression $K_C = \exp(\Delta E_{1/2}/25.69)$,[34] the comproportionation constants are 7.92

(34) See, for example: (a) Flanagan, J. B.; Margel, S.; Bard, A. J.; Anson, F. C. *J. Am. Chem. Soc.* **1978**, *100*, 4248. (b) Ito, T.; Hamaguchi, T.; Nagino, H.; Yamaguchi, T.; Kido, H.; Zavarine, I. S.; Richmond, T.; Washington, J.; Kubiak, C. P. *J. Am. Chem. Soc.* **1999**, *121*, 4625.

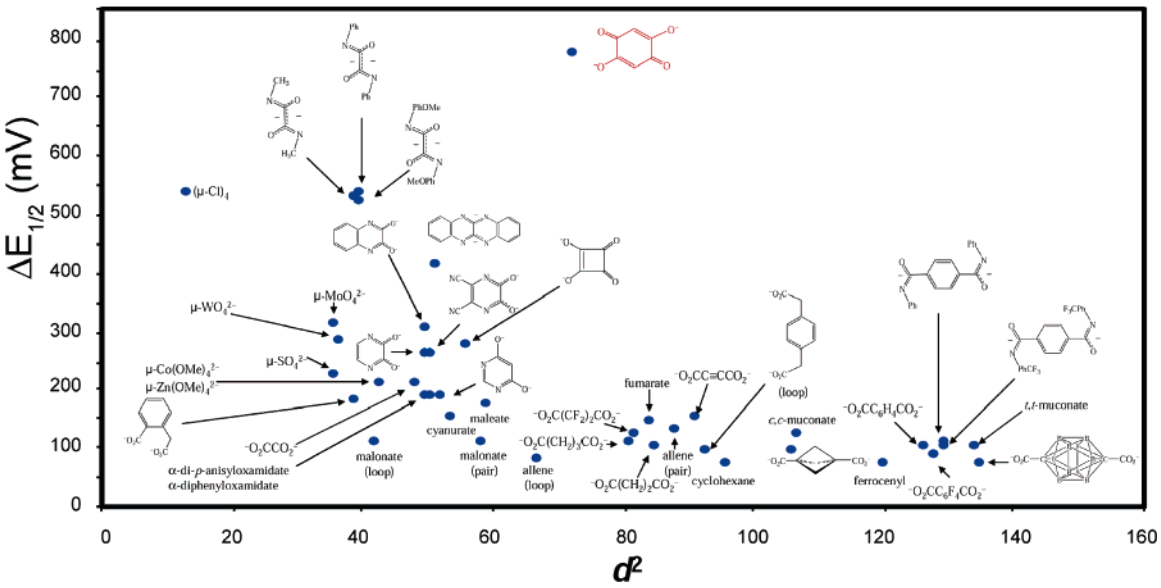

Figure 5. Distribution of $\Delta E_{1/2}$ values versus the square of the distances between midpoints of the Mo_2 units, d^2, in known $[Mo_2]L[Mo_2]$ compounds reported from this laboratory. Note that the point for dioxolene compound **1** deviates considerably from what is expected from electrostatic interactions because of the strong delocalization of electrons in this system. For simplicity, the values for **2** and **3** are not included.

$\times 10^{12}$, 2.75×10^{13}, and 6.23×10^{13} for **1**, **2**, and **3**, respectively. For M−L−M systems, it is usually stated[35] that a system with comproportionation constants above 10^6 ($\Delta E_{1/2}$ of about 350 mV) is delocalized.[36] For example, the Creutz−Taube ion, which has a $\Delta E_{1/2}$ of 390 mV, corresponding to $K_C = 3.9 \times 10^6$, is often considered to be a delocalized species,[1f] although structural support for this is lacking.[37] The large values for compounds **1** and **2** support the idea that the MV species **4** and **5** belong to Class III. It should be noted that, in the present case, there is structural data to show that the two Mo−Mo distances in each of the cations are equivalent, and therefore, the assignment of the cations in **4** and **5** to Class III is unambiguous (vide infra).[38]

It is important to note also that the distance between the midpoints of the $[Mo_2]$ units, about 8.7 Å, in these compounds is so large that a significant direct interaction between $[Mo_2]$ units, such as that observed in hydride bridged compound $\{[Mo_2(DAniF)_3](\mu\text{-}H)_2[Mo_2(DAniF)_3]\}$,[39] can be ruled out. Therefore, the strong interaction between the $[Mo_2]$ units in these molecular pairs must be due to efficient involvement of the dioxolene linkers, as indicated by the extremely short Mo−O bond distances and the delocalized structure of the linker in the solid structure.[40] The strong interaction between the $[Mo_2]$ units and the linker provides an extensive molecular orbital to distribute the unpaired electron over the metal centers and the linker after the first oxidation. This results in a high potential for the second oxidation process. The structures of the HOMO and SOMO, as shown in Figure 3, agree with a strong interaction between the $[Mo_2]$ units and the linker and show significant contributions from the linker to both the HOMO and HOMO-1. Furthermore, the electronic structure of **1** is similar to that of anthracene.[41] A comparison of the frontier molecular orbitals of anthracene and those of **1** is shown in Figure 6. The isolobality of the anthracene HOMO-1, and LUMO and the HOMO-1 and HOMO from **1**, respectively, is noticeable. The doubly oxidized product of **1**, which was not isolated but observed electrochemically, has the same 14 π electron count as anthracene, which is aromatic. It is important to note that the delocalization of electrons involves the metal−metal bonds, as shown in Scheme 1b. This situation is unique to systems with metal−metal bonds, and it does not occur in systems with single metal atoms, such as the Creutz−Taube ion.

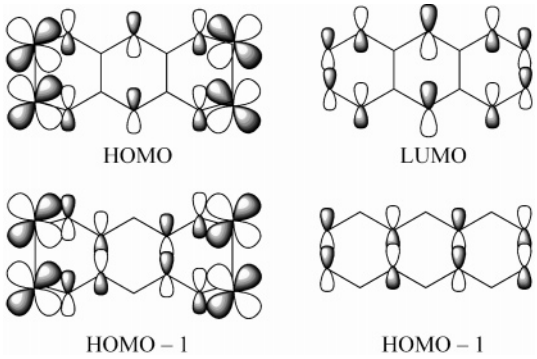

Figure 6. Diagram for the frontier orbitals for **1** (left) and anthracene (right).

For **4** and **5**, the X-band EPR spectra measured in CH_2Cl_2 at room temperature are very similar. As an example, the experimental and simulated spectra for **4** are shown in Figure 7. The data are consistent with the single electron being delocalized over four molybdenum nuclei. The *g* values of 1.938 for **4** and 1.940 for **5** are significantly lower than the free

(35) (a) Lee, M.-T.; Foxman, B. M.; Rosenblum, M. *Organometallics* **1985**, *4*, 539. (b) Atwood, C. G.; Geiger, W. *J. Am. Chem. Soc.* **2000**, *122*, 5477.
(36) It should be noted that a large separation of the redox potentials is a necessary but not sufficient condition for the strong electronic interaction, and one should be cautious in using them without additional support from other spectroscopic measurements, such as electronic spectra, EPR, or from structural data.
(37) (a) Fürholz, U.; Bürgi, H.-B.; Wagner, F. E.; Stebler, A.; Ammeter, J. H.; Krausz, E.; Clark, R. J. H.; Stead, M. J.; Ludi, A. *J. Am. Chem. Soc.* **1984**, *106*, 121. (b) Fürholz, U.; Joss, S.; Bürgi, H.-B.; Ludi, A. *Inorg. Chem.* **1985**, *24*, 943.
(38) It is important to mention that Mo−Mo distances can be measured very precisely and with a very small error. Furthermore, for the cation in **4**, the two Mo−Mo distances are crystallographically independent.
(39) Cotton, F. A.; Donahue, J. P.; Huang, P.; Murillo, C. A.; Villagrán, D. *Z. Anorg. Allg. Chem.* **2005**, *631*, 2606.
(40) Note that in molecular pairs with linkers with saturated chains, such as $[Mo_2(DAniF)_3]_2(O_2CCH_2CO_2)$, the separation between $[Mo_2]$ units is 7.647 Å and $\Delta E_{1/2}$ is only 108 mV, which corresponds to $K_C = 67$. See ref 8a.
(41) Zilberg, S.; Haas, Y.; Shalk, S. *J. Phys. Chem.* **1995**, *99*, 16558.

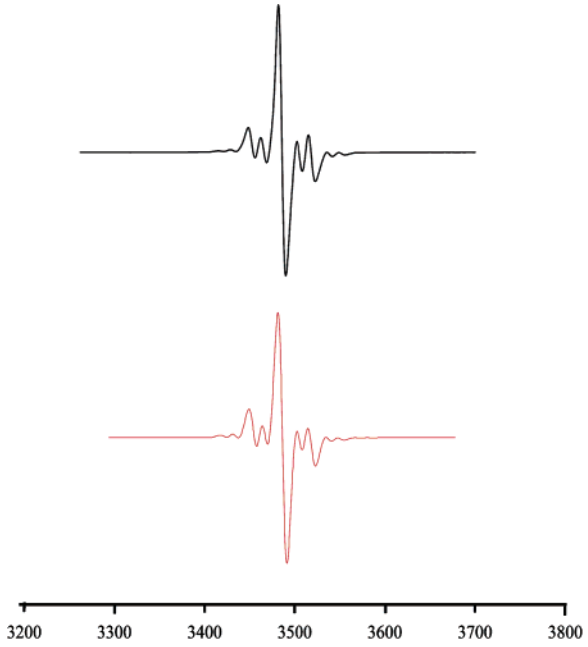

Figure 7. X-Band EPR spectrum of compound **4** in CH_2Cl_2 at room temperature (top). The simulated spectrum using $g = 1.938$, $A = 12.2 \times 10^{-4}$ cm^{-1}, and coupling with four Mo metal centers is given below the experiment spectrum. The spectrum for **5** is similar.

electron value, which results from spin−orbit coupling of the molybdenum atoms and supports the assignment of the electron removal process as being mainly a metal-based oxidation. Because of the isotope distribution of the molybdenum atoms (about 74% are ^{96}Mo atoms which have a nuclear spin I of zero; and the remaining atoms are ^{95}Mo and ^{97}Mo with $I = 5/2$ and nearly identical nuclear moments), the prominent symmetric peak in the center of each spectrum is composed mainly of overlapping signals from the species with four ^{96}Mo ($I = 0$) atoms and a sextet assigned essentially to the next most abundant mixed-valence species with two ^{96}Mo and two ^{95}Mo or ^{97}Mo. The existence of hyperfine coupling to ^{95}Mo or ^{97}Mo indicates that the unpaired electron is in a metal-based orbital. The best-fit coupling constant, 12.2×10^{-4} cm^{-1}, for both compounds is about half of that observed for $Mo_2(DAniF)_4^+$ [39] and $Mo_2(O_2CBu^t)_4^+$,[42] consistent with the extent to which electron delocalization should influence the relative magnitude of the hyperfine coupling constants.[43]

Calculations at the DFT level on a model of **4** provide additional information on the way the unpaired electron is distributed in the cations. The spin density, shown in Figure 8, indicates that the odd electron is extensively delocalized over the [Mo_2] units and the linker. The significant contribution from the linker π^* orbital in the composition of the SOMO provides an efficient route for the electronic communication between the redox centers. This is consistent with the result of EPR studies, which shows that the electron is in an orbital that has mainly metal character, but is delocalized over the four molybdenum atoms. Therefore, it is appropriate to describe these mixed-valence species approximately as [$Mo^{+0.25}Mo^{+0.25}$]L[$Mo^{+0.25}$-$Mo^{+0.25}$].

(42) Chisholm, M. H.; Pate, B. D.; Wilson, P. J.; Zaleski, J. M. *Chem. Commun.* **2002**, 1084.
(43) McCleverty, J. A.; Ward, M. D. *Acc. Chem. Res.* **1998**, *31*, 842.

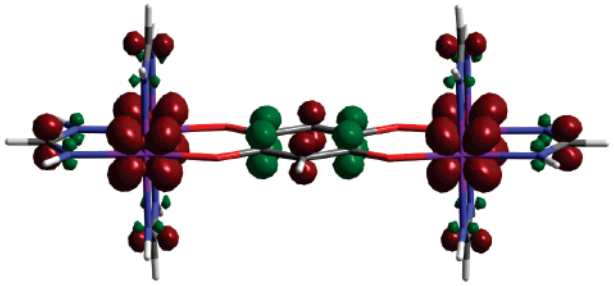

Figure 8. Illustration of the spin density of the SOMO in a model for **4**.

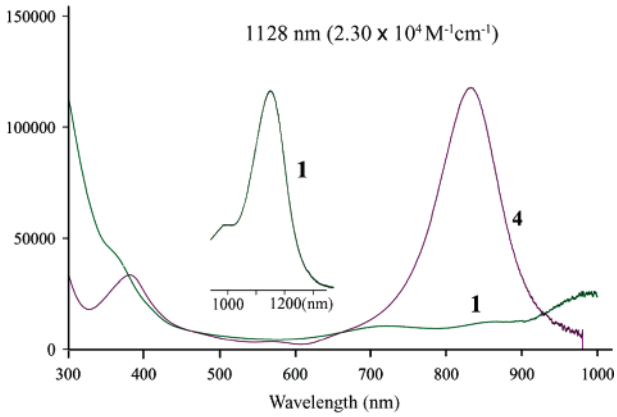

Figure 9. UV−vis spectra of **1** (in green) and **4** (in purple). The inset shows the lowest energy absorption in the NIR for **1**. The band at 1128 nm for **1** is assigned to a MLCT, while the band at 852 nm for **4** corresponds to HOMO-1 → SOMO transition.

Electronic Spectra. Up to now, all known molecular pairs having [Mo_2] units have been yellow, orange, or red. In contrast, all five compounds reported here are intensely green. The electronic spectra for **1** and **4**, shown in Figure 9, show several transitions in the visible and UV region. The most remarkable features are the low energy bands (1128 nm for **1** and 1185 nm for **2**) and those at 852 nm for **4** and at 840 nm for **5**, each with a large extinction coefficient. Time-dependent DFT calculations upon models of **1** and **4** indicate that the nature of the lowest energy bands for the neutral species and the singly oxidized one (**4**) is quite different from each other.

The absorption band at 1128 nm for **1** is the HOMO → LUMO excitation. As mentioned above, the metal contribution is large for the HOMO, while the LUMO has mainly ligand character and small metal contribution from the [Mo_2] units. Therefore, the HOMO → LUMO transition is essentially a metal-to-ligand charge-transfer band (MLCT). The charge-transfer character and the fact that this transition is allowed by symmetry give rise to a large dipole transition moment, and thus results in an intense absorption band.

The spectra of compounds **4** and **5** have particularly intense absorption bands at 852 and 840 nm for **4** and **5**, respectively. The values of $\Delta\nu_{1/2}$ (1364 cm^{-1} for **4** and 1724 cm^{-1} for **5**) are significantly less than the values predicted, 5270 and 5244 cm^{-1} for **4** and **5**, respectively, by using the Hush formula, $\Delta\nu_{1/2} = (2310\nu_{max})^{1/2}$ cm^{-1},[44] for intervalence charge-transfer bands in Class II mixed-valence compounds. This provides further evidence that these compounds are properly classified as

(44) See for example: (a) Hush, N. S. *Coord. Chem. Rev.* **1985**, *64*, 135. (b) Laye, R. H.; Couchman, S. M.; Ward, M. W. *Inorg. Chem.* **2001**, *40*, 4089. (c) Scheiring, T.; Kaim, W.; Olabe, J. A.; Parise, A. R.; Fiedler, J. *Inorg. Chim. Acta* **2000**, *300−302*, 125.

belonging to Class III. The high energy of the HOMO-1 → SOMO transition in each of the cations is consistent with the large separation between these orbitals calculated by DFT.

As shown in Figures 3 and 4, the out-of-phase δ orbital combination (b_{2g}) is stabilized by an interaction with an empty π^* orbital from the linker to form the $[Mo_2]$-based HOMO-1, while the in-phase δ combination (b_{1u}) is destabilized by interaction with an occupied π^* orbital to form the $[Mo_2]$-based HOMO. The energy gap (ΔE) between these two orbitals is a measure of the electronic interaction between the $[Mo_2]$ units.[7c,39] The calculated ΔE is 0.98 eV, which is the largest ever calculated for molecules of the $[Mo_2]L[Mo_2]$ type. For example, the calculated ΔE is 0.62 eV in the strongly coupled β-$\{Mo_2(DAniF)_3\}_2(CH_3N(O)CC(O)NCH_3)$ ($K_C = 9.5 \times 10^8$)[7c] and 0.53 eV for $\{Mo_2(DAniF)_3\}_2(\mu\text{-H})_2$ ($K_C = 8.46 \times 10^{14}$).[39] This suggests that the electronic communication in compound **4** may be stronger than in any other such molecule now known.

Conclusions

This work shows that dioxolene ligands $C_6H_2O_4^{2-}$ and $C_6Cl_2O_4^{2-}$ strongly mediate electronic communication between $[Mo_2(DAniF)_3]^+$ units. The characteristics of the neutral species **1**−**3** and the singly oxidized products **4** and **5** display a remarkable degree of electronic coupling. The mixed-valence species **4** and **5** are shown to belong to Class III of mixed-valence compounds based on the Robin−Day classification as shown by the large value (ca. 10^{12}) of the comproportionation constant (K_C), the structural equality of the Mo−Mo distances in each compound, the spectra from UV−vis and EPR spectroscopies, and DFT calculations.

In contrast to molecular pairs of mononuclear metal units with a bridging dhbq ligand, in which there is often uncertainty concerning the oxidation states of the metal atoms, the structural and spectroscopic data for compounds containing $[Mo_2]$ units allow a straightforward and unambiguous assignment. For example, the neutral species **1** may be formulated in three ways, $[Mo_2](I)(dhbq^{2-})[Mo_2](I)$, $[Mo_2](II)(dhbq^{4-})[Mo_2](II)$, and $[Mo_2](II)(dhbq^{3-})[Mo_2](I)$, where $[Mo_2](I)$ represents the species with a $\sigma^2\pi^4\delta^2$ electronic configuration and $[Mo_2](II)$ the oxidized species with a $\sigma^2\pi^4\delta$ configuration. The formula $[Mo_2](II)(dhbq^{4-})[Mo_2](II)$ can be ruled out because the linker $dhbq^{4-}$ is aromatic and would be expected to have C−C bond distances essentially identical, but is inconsistent with the large variations in such distances in **1**. Furthermore, upon a one-electron oxidation of **1**, the Mo−Mo distances increase by 0.015 Å, which is consistent with removal of an electron from a δ MO. The metal-based oxidation is further supported by EPR data. Additionally, the CV shows that there is a second metal-based oxidation that rules out the formulation $[Mo_2](II)(dhbq^{3-})[Mo_2](I)$ which would require the formation of $[Mo_2](III)$ with a $\sigma^2\pi^4$ electronic configuration, which has never been observed in species containing formamidinate ligands. Therefore, the appropriate formulation for **1** is $[Mo_2](I)(dhbq^{2-})[Mo_2](I)$.

Experimental data and calculations as well as the isolobality of the anthracene HOMO-1 and LUMO and the corresponding HOMO-1 and HOMO from the neutral species (**1**−**3**) support the formulation of such compounds as tetrametalloanthracene precursors.

Acknowledgment. We thank the National Science Foundation, the Robert A. Welch Foundation, and Texas A&M University for financial support, and the Laboratory for Molecular Simulation in this department for the software used in DFT calculations. We also thank J. P. Donahue for facilitating the files for Figure 5.

Supporting Information Available: X-ray crystallographic files in CIF format for **1**, **2**, **4**, and **5**, a figure of the core structure of **3**, and complete ref 18 in PDF (Figure S1). This material is available free of charge via the Internet at http://pubs.acs.org.

JA0582962